Bjerknes force threshold for stable single bubble sonoluminescence

I. Akhatov,* R. Mettin, C. D. Ohl,† U. Parlitz, and W. Lauterborn
Drittes Physikalisches Institut, Universität Göttingen, Bürgerstraße 42-44, D-37073 Göttingen, Germany
(Received 8 August 1996)

An investigation of the primary Bjerknes force acting on a bubble in a strong acoustic field is presented. The approach takes into account the nonlinear resonancelike response of small bubbles to strong acoustic pressure amplitudes. It is shown that for high pressure amplitudes even very small bubbles are repelled from the pressure antinode. This result is in contrast to predictions using Bjerknes forces based on harmonic bubble oscillations. The relevance of this high pressure instability for single bubble sonoluminescence experiments is discussed. [S1063-651X(97)07203-6]

PACS number(s): 47.20.Ky, 43.25.+y, 43.35.+d, 78.60.Mq

The light emission associated with strong bubble collapse in an external sound field is called *sonoluminescence* (SL). Since the work of Marinesco and Trillat [1], it has been investigated by many authors (see the review by Walton and Reynolds [2]). This type of sonoluminescence is now called *multibubble sonoluminescence* (MBSL) and generically occurs in acoustic cavitation [3–5] and sonochemistry [6–8]. The interest in SL was restimulated by the elaborate experiments of Gaitan *et al.* [9], who investigated SL of a single bubble in water trapped by a strong acoustic standing-wave field. This phenomenon is called *single bubble sonoluminescence* (SBSL) and was subsequently studied in a number of papers [10].

A prerequisite for SBSL are oscillating bubbles that remain stable in the presence of strong sound fields. Stability theories have been presented (taking into account rectified diffusion) that provide explanations for the existence of small, stably oscillating bubbles that have been observed in experiments on SBSL [11]. However, the source of the instability of SBSL occurring at even larger pressure amplitudes has not been totally clarified yet. The most popular idea presented until now considers the onset of surface oscillations to be the main mechanism leading to an instability of the bubble at the pressure antinode [12,13]. However, no theory exists connecting surface oscillation instability with trapping instability. Trapping is caused by the primary Bjerknes force and is a combined effect of the sound field and (nonlinear) bubble oscillations. In this paper we investigate the influence of the primary Bjerknes force on the positional stability of a single nonlinearly oscillating bubble in the vicinity of the pressure antinode of the levitating and driving sound field.

A body of volume V in a liquid under a pressure gradient ∇p experiences a force $\mathbf{F}=-V\nabla p$. If these quantities vary periodically in time or are fluctuating fast, the net force on the body is the time average of $\mathbf{F}$. The net radiation force acting on a spherical bubble in a standing-wave sound field is called the *primary Bjerknes force* $\mathbf{F}_B$ [3,14] and equals

$$\mathbf{F}_B=-\tfrac{4}{3}\pi\langle R^3(t)\nabla p(t)\rangle, \tag{1}$$

where $\langle\cdots\rangle$ denotes the time averaging over a period of the acoustic field.

For a quantitative investigation of the primary Bjerknes force acting on a bubble in a strong acoustic field we consider the problem in spherically symmetric geometry in a compressible liquid with forced radial excitation, i.e., a spherical bubble trap. The pressure distribution of the first radial mode, as a solution of the linear wave equation in spherical geometry, may be written in the following way:

$$p(r,t)=p_0+\frac{\sin kr}{kr}p_a(t). \tag{2}$$

Here p_0 is the initial uniform (atmospheric) pressure, $p_a(t)=-P_a\sin\omega t$ is the acoustic pressure in the center of the spherical volume with amplitude P_a, r is the radial coordinate, ω and $k=\omega/C_l$ are the frequency and the wave number of the acoustic field, and C_l is the speed of sound in the liquid. We will consider the behavior of a bubble in the close vicinity of the pressure antinode where the following approximation of the pressure distribution Eq. (2) may be used:

$$p(r,t)=p_0+\left[1-\frac{(kr)^2}{6}\right]p_a(t). \tag{3}$$

Computing the pressure gradient from Eq. (3) results in

$$\nabla p=-\tfrac{1}{3}k^2p_a(t)\mathbf{r}, \tag{4}$$

and the primary Bjerknes force Eq. (1) equals

$$\mathbf{F}_B=f_B\mathbf{r},\quad f_B=\tfrac{4}{9}\pi k^2\langle R^3(t)p_a(t)\rangle. \tag{5}$$

Close to the vicinity of the pressure antinode the primary Bjerknes force acts as a linear spring, and the "stiffness coefficient" f_B of this spring may change its sign. If $\langle R^3(t)p_a(t)\rangle$ is negative then the coefficient $f_B<0$, the Bjerknes force is directed towards the center of the spherical flask, and the bubble is trapped. If $\langle R^3(t)p_a(t)\rangle$ is positive then $f_B>0$, the bubble is repelled, and the position of the bubble in the pressure antinode is unstable.

*Permanent address: Department of Continuous Media Mechanics, Bashkir University, 32 Frunze Str., Ufa 450074, Russian Federation. Electronic address: iskander@ncan.bashkiria.su
†Electronic address: ohl@physik3.gwdg.de

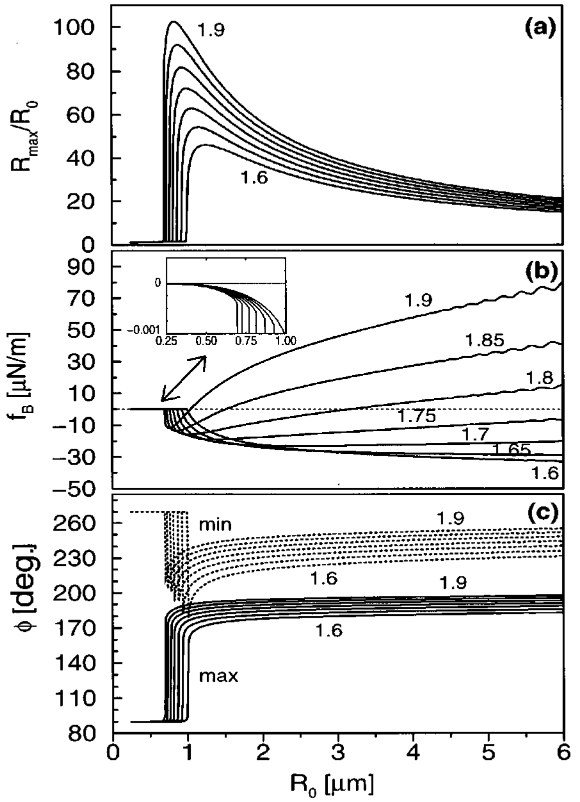

FIG. 1. (a) Response curve $R_{\max}/R_0$ vs R_0 and (b) the coefficient f_B of the primary Bjerknes force Eq. (5) vs R_0 for different pressure amplitudes $P_a=1.6$ bar to $P_a=1.9$ bar. In (c), the phases of the maximum and the minimum value of R are shown for the same pressure values.

For $P_a \ll p_0$ the bubble radius $R(t)$ oscillates as a harmonic oscillator. When plotting the ratio $R_{\max}/R_0$ vs the equilibrium radius R_0 a maximum occurs at the Minnaert resonance radius

$$R_M = \frac{1}{\omega}\sqrt{\frac{3\kappa p_0}{\rho}} \tag{6}$$

for a given frequency ω, density of the liquid ρ, and polytropic exponent κ [15]. It may be shown analytically [2,3] that a bubble of less than this linear resonance size oscillates out of phase with the sound field (that means during the positive driving pressure a reduction of the bubble volume occurs) and bubbles larger than resonance size oscillate in phase. Therefore bubbles of equilibrium radius $R_0 < R_M$ experience a negative Bjerknes force ($f_B<0$) and move towards the pressure antinode, and bubbles with $R_0 > R_M$ experience positive $\mathbf{F}_B$ and drift in direction to the pressure node.

The theory for weakly nonlinear oscillations gives a good description of the motion of bubbles in a weak stationary sound field due to the primary Bjerknes force [2,3,14,16–20]. Generally speaking the change of the sign of the primary Bjerknes force is closely correlated with the response curves that describe the dependence of the maximum size and the phase of bubble oscillations on the equilibrium radius of the bubble. Near the resonance radius the phase of the bubble oscillation changes rapidly yielding a change of the sign of the primary Bjerknes force. Because of this change in phase, linear theory predicts that all bubbles with $R_0 < R_M$ are always trapped at the pressure antinode. However, in experiments on acoustic cavitation and SBSL only bubbles that are *much smaller* than linear resonance size have been observed ($R_0 \approx 1$ μm, $R_M \approx 100$ μm, $\omega \approx 2\pi \times 20$ kHz). Recently [11] it was shown that for very small bubbles in very strong sound fields a nonlinear resonancelike behavior of the bubbles occurs that is based on the strong influence of the surface tension on the dynamics of small bubbles. In particular, it was found that this nonlinear resonance is responsible for the strongly nonmonotonous dependence of the rectified diffusion growth rate on the equilibrium bubble radius. As a consequence, these results have provided an explanation for the existence of small stably oscillating bubbles that have been observed in experiments on SL. In the following, we investigate the primary Bjerknes force acting on a small strongly nonlinear oscillating bubble in the case of this resonance, which occurs for R_0 far less than R_M.

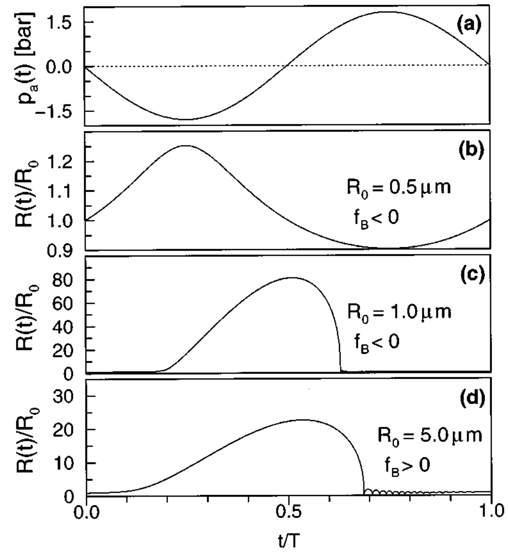

FIG. 2. Bubble oscillations for different equilibrium radii R_0. Plotted is one period $T=2\pi/\omega$ of the oscillation for a pressure amplitude of $P_a=1.8$ bar. Sound field pressure $p_a(t)$ vs t/T (a) and normalized bubble radius $R(t)/R_0$ vs normalized time t/T for $R_0=0.5\mu$m (b), $R_0=1$ μm (c), and $R_0=5$ μm (d). For (b) and (c) the primary Bjerknes force is attracting and for (d) repulsive.

The results given in the following figures have been computed using the Keller-Miksis model [21]:

$$\left(1-\frac{\dot{R}}{C_l}\right)R\ddot{R}+\frac{3}{2}\dot{R}^2\left(1-\frac{\dot{R}}{3C_l}\right)=\left(1+\frac{\dot{R}}{C_l}\right)\frac{p_l}{\rho}+\frac{R}{\rho C_l}\frac{dp_l}{dt},$$

with

$$p_l=\left(p_0+\frac{2\sigma}{R_0}\right)\left(\frac{R_0}{R}\right)^{3\kappa}-p_0-\frac{2\sigma}{R}-\frac{4\mu}{R}\dot{R}-p_a(t)$$

for air bubbles in water at 20 °C with $\kappa=1.4, \sigma=0.0725$ N/m, ρ=998 kg/m^3, μ=0.001 Ns/m^2, $p_0=1$ bar,

$C_l = 1500$ m/s, and a driving frequency of $\omega = 2\pi \times 20$ kHz. Qualitatively the same results have been obtained for the Gilmore model [22].

Figure 1(a) shows response curves for different values of the pressure amplitude P_a. The ''stiffness coefficient'' f_B of the primary Bjerknes force, Eq. (5), was calculated numerically for different equilibrium radii R_0 and different pressure amplitudes P_a. The results are shown in Fig. 1(b). For very small R_0 (before the resonance response occurs) the Bjerknes force is very small and negative [$f_B < 0$, see inset in Fig. 1(b)]. When increasing the equilibrium radius the response of the bubble increases rapidly leading to a strong amplification of the Bjerknes force. For medium P_a the coefficient of the Bjerknes force f_B depends on R_0 monotonically, but for $P_a > 1.65$ bars the quantity f_B starts to depend on R_0 nonmonotonically and for certain values of $R_0 = R_0^{\rm crit}(P_a)$ the Bjerknes force changes sign and becomes repulsive. This means that for very strong amplitudes of the acoustic field only very small bubbles [$R_0 < R_0^{\rm crit}(P_a)$] are trapped in the pressure antinode. The larger bubbles will be repelled because their position in the center of the flask becomes unstable. *This positional instability cannot be predicted by the analysis of linear bubble oscillations, because the equilibrium radius R_0 is smaller than R_M.*

To understand the reason for this change in sign of the Bjerknes force, in Figs. 2(b)–2(d) a single cycle of a typical bubble oscillation is presented for different equilibrium radii R_0. Figure 2(a) shows the driving pressure of the external sound field, $p_a(t) = -P_a \sin(\omega t)$, at the center of the bubble trap for $P_a = 1.8$ bars. It can be seen that for very small bubbles [Fig. 2(b)] the surface tension pressure $P_\sigma = 2\sigma/R_0$ is very high and the bubbles behave like flexible particles oscillating nearly sinusoidally out of phase with the driving pressure. Therefore (as mentioned above) it follows from linear theory that the sign of the Bjerknes force is negative ($R_0 = 0.5$ μm, $f_B = -6 \times 10^{-5} \mu$N/m). For larger bubbles they start to oscillate differently: the expansion grows enormously. By that, the magnitude of the Bjerknes force increases 10^6 times (because $R_{\rm max}$ increases 100 times), but it is still attractive to the center of the flask. This case is shown in Fig. 2(c) ($R_0 = 1 \mu$m, $f_B = -16$ μN/m). By further increasing R_0 the magnitude and sign of the Bjerknes force depend on the phase of the bubble collapse relative to the phase of the driving pressure. It can be seen in Fig. 2(d) ($R_0 = 5 \mu$m, $f_B = 9.6$ μN/m) that, when increasing the equilibrium radius, the instant of the bubble collapse moves constantly deeper into the compression part of the driving period [see Fig. 2(c)]. This leads to a change in sign of the Bjerknes force at some threshold value of the equilibrium radius, $R_0^{\rm crit}$.

In Fig. 3 this threshold value $R_0^{\rm crit}$ of the equilibrium bubble radius is shown versus the pressure amplitude P_a. For sufficiently low pressure amplitude all small bubbles are trapped in the pressure antinode. At higher pressures P_a a (small) critical equilibrium radius $R_0^{\rm crit}(P_a)$ exists such that all bubbles with $R_0 > R_0^{\rm crit}(P_a)$ will be repelled from the center of the flask.

For lower pressure amplitudes P_a than given in Fig. 3 the curve $R_0^{\rm crit}(P_a)$ no longer stays monotonous but attains a very complicated shape with bends and folds according to the nonlinear resonances of the different bubbles. In this region of the parameter space the dependence of $R_0^{\rm crit}$ on P_a cannot be described anymore by a single curve due to the occurrence of coexisting attractors governing the driven bubble oscillations that even may become chaotic [23]. A detailed account of this complex stability structure is beyond the scope of this paper and will be given elsewhere.

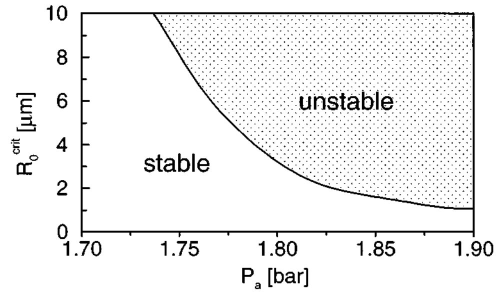

FIG. 3. Critical equilibrium radius $R_0^{\rm crit}$ vs pressure amplitude P_a. The curve separates the stable parameter region where bubbles are trapped from the unstable one.

The investigations presented in this Brief Report have shown that the critical radius where the Bjerknes force changes its sign is shifted towards smaller radii in the case of strongly nonlinear oscillations due to very high sound field amplitudes. In the context of SBSL this effect may lead to a selection mechanism where only sufficiently small bubbles can be trapped at the pressure antinode of the experimental setup (flask). On the other hand, such small bubbles either dissolve or become unstable due to rectified diffusion if the amplitude of the sound field is sufficiently high. The bubbles grow to a new larger value where they are stable from the diffusion point of view [11] but are repelled from the center due to the primary Bjerknes force.

Therefore, no bubbles can be trapped stably by the action of the primary Bjerknes force alone, when a certain threshold of the pressure amplitude is exceeded regardless of other effects that may lead to separate thresholds, e.g., surface oscillations. An upper pressure threshold indeed is observed in experiments on SBSL [9] and is usually interpreted in terms of unstable surface oscillations [12,13]. However, it should be noted that the stability threshold for surface oscillations obviously is not synonymous with a trapping threshold. Experiments show that bubbles stay trapped at pressure values *above* the theoretically predicted ones for the onset of surface oscillations. This is to be expected because a bubble destroyed by surface oscillations necessarily ends up in a number of smaller bubbles that, individually looked at, should either dissolve or grow again due to rectified diffusion, but stay trapped. Only a very involved theory considering the interaction of small bubble clusters could give a real estimate of a trapping threshold due to surface oscillations.

The trapping threshold due to primary Bjerknes forces as presented here is, to our knowledge, larger than observed so far in experiments. Besides the idea of surface oscillations (where there exists no final theory yet) a number of other reasons can be put forward to account for a lower threshold than given by the primary Bjerknes force for nonlinearly oscillating bubbles. The bubble emits shock waves that are reflected from the walls of the container. Experiments are done in cylindrical and spherical flasks that exhibit different focusing properties after reflection at the walls. Thus the driving is not purely sinusoidal as assumed in the theoretical model. And it may not be spherically symmetric either. Thus the threshold may be increased by careful experimentation. But according to our theory, it cannot be increased beyond the absolute limit given in Fig. 3.

The nonlinear features of the primary Bjerknes force presented in this Brief Report are not only significant for understanding experiments on sonoluminescence. They are also important for structure formation processes that occur in strong acoustic fields and lead to complex filamentary bubble clusters [24].

Note added. Recently we became aware through L.A. Crum of the work of S.M. Cordry addressing the same problem: Bjerknes Forces and Temperature Effects in Single Bubble Sonoluminescence, Ph.D. thesis, University of Mississippi, 1995

This work was supported by the Projektträgerschaft Internationales Büro (Contract X222.31), the Ministry for Science, Higher Education and Technical Policy of the Russian Federation and the State Committee of the Russian Federation for Higher Education.

[1] N. Marinesco and J. J. Trillat, Proc. R. Acad. Sci. **196**, 858 (1933).

[2] A. J. Walton and G. T. Reynolds, Adv. Phys. **33**, 595 (1984).

[3] F. R. Young, *Cavitation* (McGraw-Hill, London, 1989); T. G. Leighton, *The Acoustic Bubble* (Academic Press, London, 1994).

[4] H. Kuttruff, Acustica **12**, 230 (1962).

[5] C. D. Ohl, H.-C. Nägerl, R. Blatt, and W. Lauterborn, *DAGA - Fortschritte der Akustik*, edited by T. Porterle and W. Hess (DEGA e.V., Oldenburg, 1996), pp. 418, 419.

[6] *Ultrasound: Its Chemical, Physical, and Biological Effects*, edited by K. S. Suslick (VCH Publishers, New York, 1988).

[7] *Advances in Sonochemistry, Vol. 1*, edited by T. J. Mason (JAI Press, Hampton Hill, 1990).

[8] K. S. Suslick, Science **247**, 1439 (1990).

[9] D. F. Gaitan, L. A. Crum, C. C. Church, and R. A. Roy, J. Acoust. Soc. Am. **91**, 3166 (1992); D. F. Gaitan, Ph.D. thesis, University of Mississippi, 1990 (unpublished).

[10] B. P. Barber and S. J. Putterman, Nature (London) **352**, 318 (1991); R. Hiller, S. J. Putterman, and B. P. Barber, Phys. Rev. Lett. **69**, 1182 (1992); R. Löfstedt, B. P. Barber, and S. Putterman, Phys. Fluids A **5**, 2911 (1993); L. A. Crum, Physics Today **47** (No. 9), 22 (1994); R. G. Holt, D. F. Gaitan, and J. Holzfuss, Phys. Rev. Lett. **72**, 1376 (1994); B. P. Barber, K. Weninger, R. Löfstedt, and S. Putterman, *ibid.* **74**, 5276 (1995).

[11] R. Löfstedt, K. Weninger, S. Putterman, and B. P. Barber, Phys. Rev. E **51**, 4400 (1995); M. P. Brenner, D. Lohse, D. Oxtoby, and T. F. Dupont, Phys. Rev. Lett. **76**, 1158 (1996); I. Akhatov, N. Gumerov, C. D. Ohl, U. Parlitz, and W. Lauterborn, *ibid.* **78**, 227 (1997).

[12] M. P. Brenner, D. Lohse, and T. F. Dupont, Phys. Rev. Lett. **75**, 954 (1995); A. I. Eller and L. A. Crum, J. Acoust. Soc. Am. **47**, 762 (1969).

[13] H. W. Strube, Acustica **25**, 289 (1971).

[14] F. G. Blake, Jr., J. Acoust. Soc. Am. **21**, 551 (1949).

[15] M. Minnaert, Philos. Mag. **16**, 235 (1933).

[16] T. G. Leighton, A. J. Walton, and M. J. W. Pickworth, Eur. J. Phys. **11**, 47 (1990).

[17] D. L. Miller, J. Acoust. Soc. Am. **62**, 12 (1977).

[18] L. A. Crum and A. I. Eller, J. Acoust. Soc. Am. **48**, 181 (1969).

[19] L. A. Crum, J. Acoust. Soc. Am. **57**, 1363 (1975).

[20] *Cavitation and Inhomogeneities in Underwater Acoustics*, edited by W. Lauterborn (Springer, Berlin, 1980).

[21] J. B. Keller and M. Miksis, J. Acoust. Soc. Am. **68**, 628 (1980).

[22] F. R. Gilmore, Hydrodynamics Laboratory, California Institute of Technology, Pasadena, California, Report No. 26-4, 1952 (unpublished).

[23] W. Lauterborn and E. Cramer, Phys. Rev. Lett. **47**, 1445 (1981); W. Lauterborn and E. Suchla, *ibid.* **53**, 2304 (1984); W. Lauterborn and U. Parlitz, J. Acoust. Soc. Am. **84**, 1975 (1988); U. Parlitz, V. Englisch, C. Scheffczyk, and W. Lauterborn, *ibid.* **88**, 1061 (1990).

[24] I. Akhatov, U. Parlitz, and W. Lauterborn, J. Acoust. Soc. Am. **96**, 3627 (1994); U. Parlitz, C. Scheffczyk, I. Akhatov, and W. Lauterborn, Chaos, Solitons Fractals **5**, 1881 (1995); I. Akhatov, U. Parlitz, and W. Lauterborn, Phys. Rev. E **54**, 4990 (1996).